JACS
JOURNAL OF THE AMERICAN CHEMICAL SOCIETY
Article
pubs.acs.org/JACS

Length-Dependent Conductance of Oligothiophenes

Brian Capozzi,[†,§] Emma J. Dell,[‡,§] Timothy C. Berkelbach,[‡] David R. Reichman,[‡] Latha Venkataraman,*[,†] and Luis M. Campos*[,‡]

[†]Department of Applied Physics and Mathematics, Columbia University, New York, New York 10027, United States
[‡]Department of Chemistry, Columbia University, New York, New York 10027, United States

Supporting Information

ABSTRACT: We have measured the single-molecule conductance of a family of oligothiophenes comprising 1−6 thiophene moieties terminated with methyl-sulfide linkers using the scanning tunneling microscope-based break-junction technique. We find an anomalous behavior: the peak of the conductance histogram distribution does not follow a clear exponential decay with increasing number of thiophene units in the chain. The electronic properties of the materials were characterized by optical spectroscopy and electrochemistry to gain an understanding of the factors affecting the conductance of these molecules. We postulate that different conformers in the junction are a contributing factor to the anomalous trend in the observed conductance as a function of molecule length.

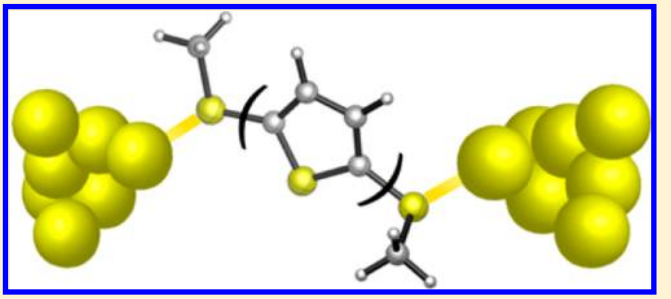

INTRODUCTION

Poly- and oligothiophenes are ubiquitous throughout organic electronic devices including photovoltaics and thin-film transistors.[1] This prevalence stems from their favorable chemical stability and synthetic versatility, together with outstanding optoelectronic properties.[1a] However, understanding the structural and electronic building blocks, from oligomers to polymers, that specifically contribute to their overall performance remains a challenge. There is a need to enlarge the set of characterization tools in order to enable the detailed understanding of the structure−property relationship of organic semiconductors.[2] Recently, Briseño and co-workers demonstrated the effect of conjugation on bulk conduction properties,[3] while Smith and co-workers studied solid-state thermal properties.[4] Oligothiophenes (OTs) have received little attention in the realm of single-molecule studies.[5] While a small number of research groups have demonstrated that oligothiophenes are conducting,[5b,6] a thorough investigation of the relationship between molecular structure and conductance is lacking in these systems, and the idea of using single-molecule studies as a tool for characterizing the building blocks that constitute macromolecules remains in its infancy. Here, we probe the electronic characteristics of a series of bare OTs, which contain gold-binding linkers directly on the thiophene moieties, by measuring their conductance in metal-molecule-metal junctions. In this work, we uncover an unusual length-dependent conductance for the oligothiophenes, and we focus on understanding the unexpectedly high conductance of quaterthiophene.[5a] We demonstrate how these single-molecule measurements can reveal unexpected electronic structure features of the molecules that are not observed in bulk measurements, and we describe our efforts to probe the origin of this unusual conductance trend.

To our knowledge, the most fundamental and needed study of the single molecule conductance length dependence of OTs has not been carried out. In particular, previous studies of OTs contained gold-binding linkers separated by aliphatic units[5a,c] or functional groups along the backbone,[7] which can affect conformation and electronic properties. Tada and co-workers have probed the conductance of long oligothiophene molecular wires, surrounded by alkylsilyl groups,[7b,c] starting at five repeat units, and have recently synthesized wires completely encapsulated by fluorene units.[7a] Tao and co-workers compared the conductance properties of ter- and quaterthiophene analogues.[5a] They demonstrated, as we also observe, that the latter shows a higher conductance, and they attribute this to its highest occupied molecular orbital (HOMO) level being better aligned with the Fermi level of gold. Motivated by this result, and keeping in mind that the reduced symmetry of thiophenes leads to a broad distribution in conductance histograms,[8] we have carried out a thorough evaluation of the family of OTs to shed light on this anomalous behavior.

RESULTS AND DISCUSSION

In order to probe charge transport through oligothiophenes and understand how transport scales with length, we synthesized a family of compounds containing 1−6 thiophene units with gold-binding methyl sulfide end groups—the most fundamental family in its class to be studied in single molecule junctions (Figure 1a). The molecules were synthesized by

Received: May 26, 2014

   dx.doi.org/10.1021/ja505277z | J. Am. Chem. Soc. XXXX, XXX, XXX−XXX

palladium-catalyzed cross-coupling chemistries[9] and fully characterized by standard techniques.

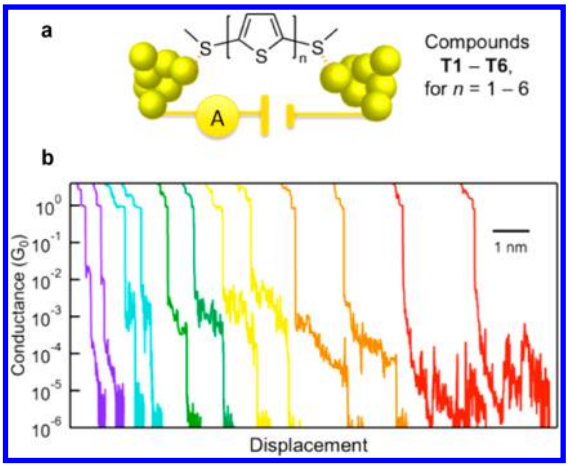

Figure 1. (a) Schematic of the scanning tunneling microscope break-junction (STM-BJ) technique used to measure the conductance of oligothiophenes. (b) Sample STM-BJ conductance traces for T1−T6 carried out under a bias voltage of 90 mV for T2, 220 mV for T3−T5, and 500 mV for T6. Note: T5 and T6 have hexyl chains for solubility, which are omitted here for clarity.

The scanning tunneling microscope break-junction (STM-BJ) technique was used to measure the conductance of T1−T6.[10] Single-molecule junctions are formed by repeatedly driving a gold tip into and out of contact with a gold-coated mica substrate; as the tip is retracted, an atomic point contact is formed and subsequently broken, creating a gap small enough to accommodate a gold-binding molecule. The measurements are carried out in solution of 1,2,4-trichlorobenzene (TCB, 10 μM to 1 mM concentration), at ambient conditions. Additionally, other solvents were used to study and confirm that the conductance traces correspond to individual molecules, and the results will be described below. We collected thousands of traces (conductance vs displacement) that exhibit plateaus at integer multiples of the quantum of conductance, G_0 ($2e^2/h$), in addition to a plateau-like feature at below 1 G_0 that is attributed to the conductance of the molecule that bridges the ruptured gold point-contacts (Figure 1b). In general, the plateau length correlates with the length of the molecules present in solution.[11]

Compiling the thousands of single-molecule conductance traces into logarithmically binned one-dimensional histograms yields a distribution of conductance values peaked at the most frequently measured conductance (Figure 2a).[12] We note that linear-binned histograms show broad features where the peak value of conductance is not easily determined (Figure S1, Supporting Information). The width of the peaks indicates that conductance varies significantly from junction to junction and as a function of elongation. The breadth of the plots in Figure 2a can generally be attributed to the reduced symmetry of thiophenes as compared with oligophenyls, which has been previously observed in bithiophene.[8] The conductance peak for each oligomer was fit with a Gaussian to determine the most probable conductance value, as indicated by the arrows in Figure 2a and Figure S2 (Supporting Information). These values are plotted against the distance, L, between the S atoms of the methyl sulfide groups on each of the fully elongated oligothiophenes (Figure 2b).

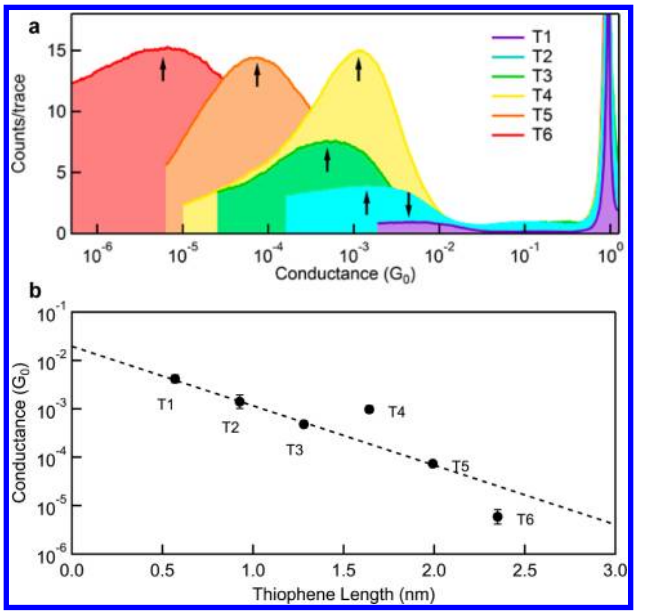

Figure 2. (a) Log-binned conductance histograms of the oligothiophenes T1−T6 (100 bins/decade). (b) Plot of conductance as a function of the length of the molecules T1−T6. Conductance for T1−T3, T5 have a decay constant $\beta = 0.29$ Å^{-1}, and T4 and T6 are clearly off this line. Error bars indicate variation in conductance peak position determined from successive measurements.

Our results show an unusual conductance trend in Figure 2b: we do not see a clear exponential decrease of conductance with oligomer length, as would be expected for coherent tunneling. The shorter (T1−T3 and T5) fall on an exponential (i.e., $G \sim e^{-\beta L}$) with a decay constant of 0.3 Å^{-1}, a value that is close to that of other conjugated systems.[13] However, T4 appears to have a higher conductance than T3, and T6 has a conductance that is lower than would be expected from a simple exponential decay. This result is in contrast to measurements of alkanes[14] or oligoenes,[13c,15] where the conductance of oligomers can be fit with a single exponential. Thus, understanding the nature of such unprecedented behavior could shed light on the factors that affect oligothiophene-based molecular junctions and can also explain the conjugation length observed in polymeric versions of this molecule.

As discussed, a higher conductance for T4 as compared to T3 has also been observed before.[5a] Since this behavior was attributed to the HOMO of quaterthiophene being closer to the gold Fermi level than that of terthiophene, we have performed cyclic voltammetry (CV) and UV−vis absorption measurements on T2−T6 in order to determine the frontier energy levels of the oligomers (Figure 3). The HOMO was determined from the oxidation potential (E_{ox}) by CV, and the lowest unoccupied molecular orbital (LUMO) was deduced from E_{ox} and the optical energy gap at the wavelength absorption onset from the UV−vis spectrum. We observe that the changes in the HOMO energy as the number of thiophenes increases are fairly small, indicating that the anomalously high conductance may not solely be due to changes in the energy level alignment of T4. In fact, T5 and T6 show almost the same oxidation potential as T4, which suggests that the HOMO does not get significantly closer to the Fermi level as the molecule length is increased. Had this been the trend that explains the anomaly, we would expect T5 and T6 to display conductance

dx.doi.org/10.1021/ja505277z | J. Am. Chem. Soc. XXXX, XXX, XXX−XXX

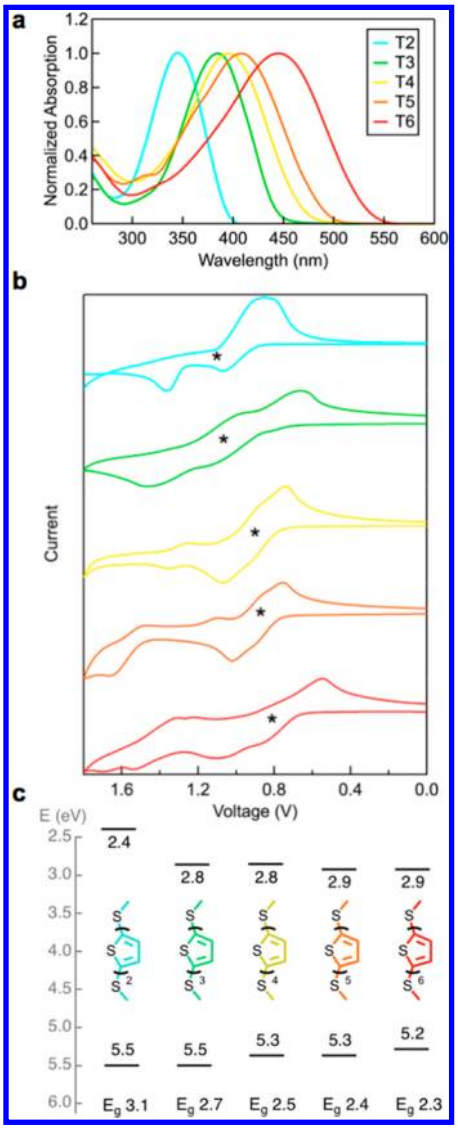

Figure 3. (a) Solution UV−vis absorption spectra of T2−T6 dissolved in DCM. (b) Cyclic voltammograms performed in dichloromethane (DCM) with Ag/AgCl reference electrode, 0.1 M tetrabutyl ammonium hexafluorophosphate as the electrolyte and a scan rate of 50 mV s^{-1} for T2−T6. Asterisks denote the position of the first oxidation potential for each molecule. (c) Optical gaps determined from UV−vis spectra placed relative to the HOMO obtained from the cyclic voltammetry following standard published methods.[16]

values similar to (or larger than) that of T4, contrary to what is seen experimentally.

Further insight into this hypothesis can be obtained from a coherent tunneling model. Since these molecules conduct through the HOMO, we construct a simplified Hamiltonian describing an oligomeric molecule (M) with N bridge sites, each representing the HOMO of a single thiophene unit (N = 1−6 for T1−T6) to elucidate the effect of increasing molecular length on the transmission characteristics (the linker gateway state is neglected for simplicity). The Hamiltonian also includes the coupling to the left (L) and right (R) gold electrodes. Specifically, we use $H = H_L + H_R + H_M + H_{ML} + H_{MR}$, with

$$H_M = \sum_{n=1}^{N} \varepsilon_H |n\rangle\langle n| + \sum_{n=1}^{N-1} t_H(|n\rangle\langle n+1| + \mathrm{HC})$$

$$H_L + H_R = \varepsilon_s(|L\rangle\langle L| + |R\rangle\langle R|)$$

$$H_{ML} + H_{MR} = t_s(|L\rangle\langle 1| + |N\rangle\langle R|) + \mathrm{HC}$$

where HC denotes the Hermitian conjugate of preceding terms. In the above equation, ε_s is the gold s-orbital energy, t_s is the coupling between the molecule and the gold, ε_H is the single-site HOMO energy, and t_H is the intersite HOMO coupling. The model system is shown schematically in Figure 4a. The

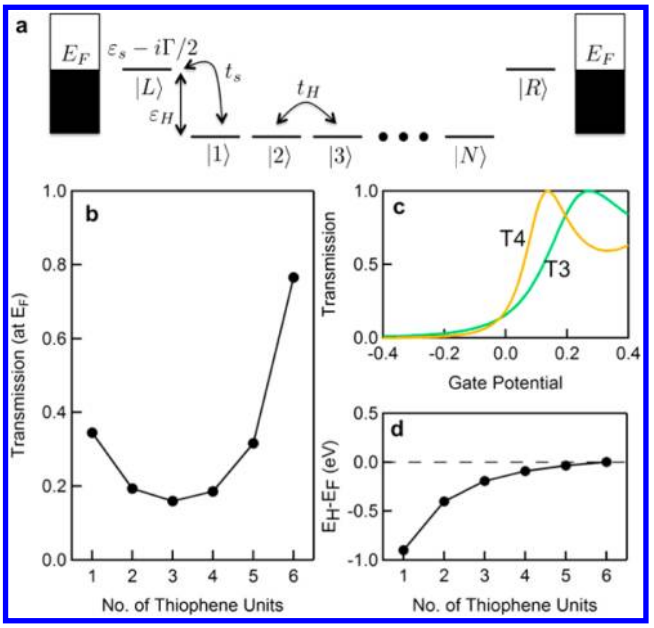

Figure 4. (a) Schematic of the tunneling model employed for transport calculations. (b) Calculated low-bias transmission, showing qualitatively correct behavior for T1−T4, but not T5 and T6. (c) Calculated gating dependence of the transmission for T3 and T4. (d) Difference in energy between the molecular HOMO and the Fermi energy of the gold electrodes.

transmission coefficient, $T(E)$, can be evaluated by standard Green's function techniques (see Methods), accounting for hybridization with the electrodes via an imaginary constant self-energy, $\Sigma = -i\Gamma/2(|L\rangle\langle L| + |R\rangle\langle R|)$.

Using reasonable approximations for the HOMO electronic coupling and the electrode hybridization (see Methods), we considered the effect of varying the offset between the HOMO site energies and the electrode Fermi energy. Through this procedure, we are simply seeking to identify a regime where we can observe an increased conductance for T4 compared to T3. When far from resonance, the transmission coefficient displays purely exponential behavior with the number of bridge sites, as typically observed.[17] By raising the HOMO site energy, one can realize a situation whereby the transmission decays for T1−T3, but increases for T4, as observed experimentally (Figure 4b). The parameters required for this behavior also qualitatively reproduce the gating dependence observed by Tao and co-workers for T3 and T4 (Figure 4c). However, this resonance effect persists for T5 and even more so for T6, predicting a continued increase in the conductance, contrary to what is seen experimentally. This behavior can be understood by tracking the molecule's HOMO energy E_H (not to be confused with ε_H) as a function of length, which demonstrates the increased resonance for T5 and T6 (Figure 4d). The evolution of the molecular HOMO energy is seen to be in good agreement with

dx.doi.org/10.1021/ja505277z | J. Am. Chem. Soc. XXXX, XXX, XXX−XXX

the CV results (Figure 3c). However, the lack of agreement between the measured and predicted conductance trends for T3−T6 indicate that in a molecular junction, the HOMO is not getting significantly closer to E_F. Thus, transport in these systems is due to a far off-resonance tunneling mechanism. In this regime, small changes in the location of E_H relative to E_F have a negligible impact on the trend in conductance as a function of molecular length. The simple model presented here fails to explain the data, confirming our proposition that the experimental behavior is not due to enhanced resonance effects.

A second possible explanation for the nonexponential decay in conductance seen here could be due to a water gating effect. Recent studies show that water solvation shells around the backbone of a molecule can change transport resonances and therefore increase conductance; this effect was found to be particularly strong for long molecules.[6a] To investigate whether the high conductance observed for T4 is a result of such a gating effect, we measure the conductance of T4 in an argon environment. We find that the conductance of T4 in argon is slightly higher than that in air (Figure S3, Supporting Information), but within the width of the histograms. Therefore, water gating cannot explain the higher conductance of T4 compared to T3 that we observe in our measurements.

It has been postulated that oligothiophenes may form pi-aggregates in solution, and Tada and co-workers have synthesized oligomers bearing groups that can hinder such aggregation.[18] However, OTs are known to pack in a herringbone structure in the solid-state, and such a packing would not enhance the conductance of molecular junctions.[19] Nonetheless, we investigated whether the molecules formed aggregates in solution by studying the temperature, concentration, and solvent dependence on their UV−vis absorption spectra. Solutions of the oligothiophenes in TCB (the solvent used for the conductance measurements) were cooled from 55 to 17 °C (Figure 5a and Figure S4, Supporting Information). During cooling, we saw no change (bathochromic or hypsochromic) in the onset of absorption of the oligothiophenes. Solutions of aggregates typically show reductions in their extinction coefficients and blue shifts on the order of 50 nm upon cooling.[20] Thus, our spectra are indicative of free molecules in solution. Changes in concentration should also affect the spectra of aggregates. We varied the concentration of oligothiophene in TCB and again saw no change in the positions of the onset of absorption or λ_{max} (Figure 5b). Molecules prone to aggregation display different behavior in "good" and "poor" solvents. When the solvent is varied, we note only a slight change in the onset of absorption and λ_{max} from the nonpolar tetradecane (C14) to the slightly polar DCB (Figure 5c). However, these changes, on the order of 5−10 nm, are minor compared to those of 50−70 nm reported as evidence of oligothiophene aggregates in solution.[20a] Furthermore, there is no change in the shape of the absorption curve, even across a wide range of solvents (Figure S5, Supporting Information), and these curves are typical for fully dissolved oligothiophenes. We also measured the conductance of T4 in various solvents and at various concentrations and saw no difference in the width of the histograms (Figure 5d and Figure S6, Supporting Information). Thus, we can rule out the possibility that pi-stacked aggregates are formed in the junction, and we cannot attribute the unusual decay trend to the sampling of multiple molecules or aggregates in the junction.

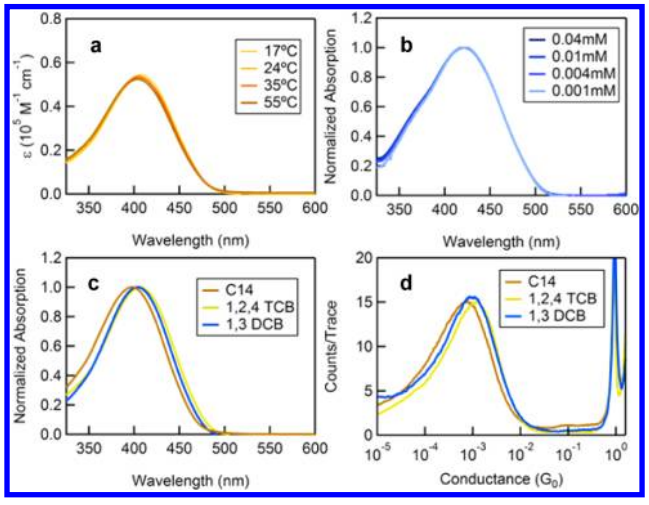

Figure 5. (a) UV−vis absorption data taken in 1,2,4-trichlorobenzene (TCB) for T4 at temperatures from 17 to 55 °C. (b) UV−vis absorption data taken in TCB for T5 at different concentrations, normalized to allow comparison of the onset of absorption. (c) UV−vis absorption data of T4 taken in different solvents. (d) Conductance histograms for T4 in three solvents: tetradecane (C14), 1,2,4-trichlorobenzene (TCB), and 1,2-dichlorobenzene (DCB).

Having ruled out HOMO-Fermi level resonance, water gating, and aggregation as explanations for the high conductance of T4, we further analyzed two-dimensional (2D) conductance histograms to extract information on the length dependent behavior, which can correlate to conformational changes, on the conductance of the oligothiophene family. Since the length of the thiophene in the junction can depend on the orientation of the thiophene units relative to each other, we constructed 2D conductance-displacement histograms, without data selection to understand how the molecular conductance evolves with junction elongation.[11] Figure 6a shows these 2D histograms for T3, T4 and T5 (others are shown in Figure S7, Supporting Information). In these plots, we see a conductance feature that extends to longer displacements with increasing number of thiophene units (Figure S8, Supporting Information). This indicates that the conductance plateau length in individual traces scales with the molecular length of the backbone, as has been found in other STM-BJ experiments.[11,21] These results thus provide additional conclusive evidence that stable molecular junctions are formed with these oligothiophenes. Furthermore, a detailed comparison of the 2D histograms for T3 and T4 (Figure 6a) indicates that the conductance of T4 is high for small displacements (relative to the point where the Au contact breaks). It is possible that for T4, the π-system couples directly to the gold electrodes at small electrode separation,[13c] enhancing conductance, though it is not clear why T5 does not show a similar effect. The 2D histograms also show that the conductance of a fully elongated T4 junction is comparable to that of a T3 junction.

To isolate and analyze the data of fully extended junctions, we determined the conductance from a subset of the two-dimensional histograms within a 0.5 nm window demarcated by the dashed lines in Figure 6a. We integrated all counts within this window to generate a conductance profile[22] (shown in the last panel of Figure 6a) and fit a Gaussian to determine a peak conductance value. These values are plotted against molecular length in Figure 6b, which is fit to a single decay with $\beta = 0.4$ Å^{-1}. However, we again see that T4 lies above the line and T6

dx.doi.org/10.1021/ja505277z | J. Am. Chem. Soc. XXXX, XXX, XXX−XXX

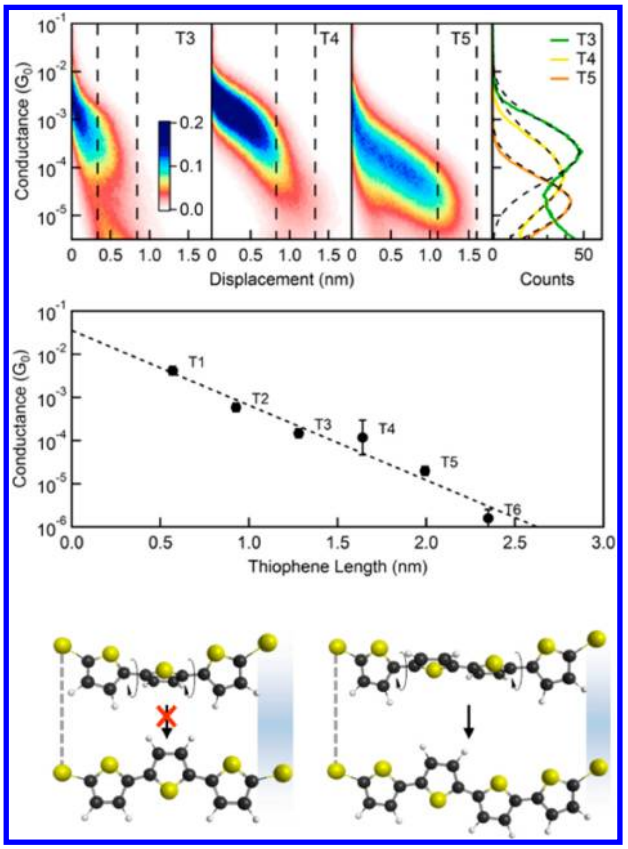

Figure 6. (a) Two-dimensional (2D) conductance histograms of T3, T4 and T5, along with the respective conductance profiles (last panel) generated from the indicated 0.5 nm windows. (b) Plot of the conductance obtained from the 2D plot for a fully elongated junction (demarcated by the dashed lines in (a)) as a function of the length of the molecules T1−T6. A line fit through the entire data set gives a decay constant $\beta = 0.4$ Å^{-1}. (c) Illustration of the hindered T3 rotation in a junction and the length increase (left) compared to the lower energy rotation and length conservation in T4 (right).

below. Furthermore, β has diminished, indicating that fully extended junctions have a smaller decay constant. This difference indicates strongly that the larger number of conformations that can be sampled in a fully elongated junction decreases the overall conjugation length in these oligothiophenes. Note that the decay constants determined here for T1−T3 are also different from that found by Yamada et al. (0.1 Å^{-1});[7c] however, their measurements were for alkylsilylamino-substituted oligomers of 8 or more units where conductance could be through a hopping mechanism.[5b,7b] Therefore, we see that this conductance trend is not entirely due to trapping molecular conformations that have shorter overall lengths.

We now turn to discuss the conformational effects in these molecular junctions, which have been previously shown to play an important role when comparing bithiophene to biphenylene conductance trends focusing on the difference between T3 and T4.[8] When chains of five-membered rings are bound in a junction their rotational freedom is restricted; this effect is more pronounced for T3 than T4. If a T3 molecule enters the junction in a twisted conformation, it is unable to rotate to a more conjugated, planar form, both due to the high degree of rotational strain and the increase in overall molecular length which would result in the junction rupturing, as illustrated in Figure 6c. In contrast, if a T4 molecule enters the junction in a twisted conformation, rotation to the more planar form is possible. A simultaneous rotation of the middle two rings does not change the end-to-end length significantly, avoiding junction rupture, thus leading to planar conjugated structures more feasibly than when compared with T3 (Figure 6c). Such a difference could explain the higher conductance observed for T4 when compared to T3 as well as the narrower conductance histogram (Figure 2a). Extending this argument to T5 and T6, one might expect an even narrower distribution in conductance than for T4. However, the extra thiophene units now yield multiple rotational degrees of freedom, which add extra disorder to the system, and thus the conductance distribution becomes quite broad again. Furthermore, the two hexyl groups on the T6 might also hinder a planar conformation in a junction, yielding a lower conductance than would be predicted by a simple exponential relation.

CONCLUSIONS

In summary, we have carried out single molecule conductance measurements on a family of methyl sulfide-terminated oligothiophenes using the scanning tunneling microscope-based break-junction technique. We find that the peak of the conductance histogram distribution does not follow a clear exponential decay with increasing number of thiophene units in the chain. We attribute this trend to different conformers formed in single-molecule junctions, which is supported by the narrow conductance distribution peak of T4 relative to all other oligothiophenes. We point out that although we have shown that a simple coherent tunneling model fails to explain the experimental data,[23] this picture precludes more complex effects, such as Coulomb interactions on the molecule, hopping transport, and strong electron−phonon coupling. All of these effects are to be expected in conjugated polymers, especially with increasing length. A more microscopic investigation of these effects is beyond the scope of the current work, but an interesting topic for future investigation.

METHODS

All reactions were performed in oven-dried round-bottom flasks, unless otherwise noted. The flasks were fitted with rubber septa and reactions were conducted under a positive pressure of argon, unless otherwise noted. Anhydrous solvents were obtained from a Schlenk manifold with purification columns packed with activated alumina and supported copper catalyst (Glass Contour, Irvine, CA). Stainless steel syringes or cannulae were used to transfer air- and moisture-sensitive liquids. Flash column chromatography was performed employing 32−63 μm silica gel (Dynamic Adsorbents Inc.). Thin-layer chromatography (TLC) was performed on silica gel 60 F254 plates (EMD).

Materials. Commercial reagents were used without further purification with the exception of *N*-bromosuccinimide (NBS), which was recrystallized from hot water. Commercial reagents purchased from Sigma-Aldrich include *n*-butyllithium (2.5 M in hexanes), potassium carbonate, 5,5′-dibromo-2,2′-bithiophene, 2,2′-bithiophene, 2,2′:5′,2″-terthiophene, thiophene, 3-hexylthiophene, *N*-bromosuccinimide, 2-isopropoxy-4,4,5,5-tetramethyl-1,3,2-dioxaborolane, triethylamine, 4,4′-bis-methylsulfanyl-biphenyl. Commercial reagents purchased from Strem Chemicals include tetrakis-(triphenylphosphine) palladium(0). Commercial reagents purchased from Acros Organics include tributyltin chloride, 2,5-dibromothiophene, dimethyl disulfide, 3,4-dibromothiophene, *n*-hexyl magnesium bromide.

Instrumentation. Proton nuclear magnetic resonance (^{1}H NMR) spectra and carbon nuclear magnetic resonance (^{13}C NMR) spectra were recorded on a Bruker DRX300 (300 MHz) and a Bruker DRX400 (400 MHz) spectrometer. Chemical shifts for protons are

dx.doi.org/10.1021/ja505277z | J. Am. Chem. Soc. XXXX, XXX, XXX−XXX

reported in parts per million downfield from tetramethylsilane and are referenced to residual protium in the NMR solvent ($CHCl_3$: d 7.26). Chemical shifts for carbon are reported in parts per million downfield from tetramethylsilane and referenced to the carbon resonances of the solvent ($CHCl_3$: d 77.0). Data are represented as follows: chemical shift, multiplicity (app = apparent, br = broad, s = singlet, d = doublet, t = triplet, q = quartet, m = multiplet), coupling constants in Hertz (Hz), and integration. The mass spectroscopic data were obtained at the Columbia University mass spectrometry facility using a JEOL JMSHX110A/110A tandem mass spectrometer. Absorption spectra were taken on a Shimadzu UV-1800 spectrophotometer.

*2,5-Bisthiomethylthiophene (**T1**).* The title compound was prepared according to published procedures,[24] yielding the product as a yellow oil (1.11 g, 55% yield): ^{1}H NMR (400 MHz, $CDCl_3$) d 6.90 (s, 2H), 2.48 (s, 6H); ^{13}C NMR (400 MHz, $CDCl_3$) δ 139.19, 131.03, 22.16; LRMS (APCI+) calculated for $C_6H_8S_3$ 176.32, found 175.98.

*5,5′-Bisthiomethyl 2,2′-bithiophene (**T2**).* The title compound was prepared according to published procedures,[8] yielding the product as a pale yellow solid (460 mg, 60% yield): ^{1}H NMR (400 MHz, $CDCl_3$) d 6.96 (s, 4H), 2.51 (s, 6H); ^{13}C NMR (400 MHz, $CDCl_3$) d 131.86, 123.94, 22.24; HRMS (FAB+) calculated for $C_{10}H_{10}S_4$ 258.45, found 258.78.

2-Tributylstannyl 5-thiomethyl thiophene. The title compound was prepared according to published procedures,[25] yielding the product as a dark brown oil (1.6 g, 92% yield): ^{1}H NMR (400 MHz, $CDCl_3$) δ 7.15 (d, J = 3.3 Hz, 1H), 7.02 (d, J = 3.3 Hz, 1H), 2.50 (s, 3H), 1.56 (m, 8H), 1.34 (m, 8H), 1.09 (m, 8H), 0.90 (m, 12H); ^{13}C NMR (400 MHz, $CDCl_3$) δ 141.85, 140.18, 135.51, 131.07, 28.76, 26.99, 21.76, 13.48, 10.70; HRMS (ESI+) calculated for $C_{17}H_{32}S_2Sn$ 419.28, found 419.28.

*5,5″Bisthiomethyl-2,2′:5′,2″-terthiophene (**T3**).* An oven-dried two necked 50 mL round-bottom flask and stir bar was fitted with a condenser and cooled under Ar. 2,5-dibromothiophene (433 mg, 1.79 mmol, 1 equiv) was added and dissolved in 15 mL of DMF. The solution was sparged with Ar for 20 min. Tetrakis(triphenylphosphine) palladium(0) (207 mg, 0.179 mmol, 0.1 equiv) was added, and the solution was heated to 80 °C. 2-Tributylstannyl 5-thiomethyl thiophene (1.50 g, 3.58 mmol, 2 equiv) was added dropwise, and the solution was heated at 80 °C overnight. The reaction mixture was cooled and passed through a silica plug with $CHCl_3$ and 1% triethylamine, to remove any remaining stannane. The eluent was poured into 100 mL of $CHCl_3$, washed with water (5 × 100 mL) and brine (100 mL), and dried over magnesium sulfate. After filtration, the organic layer was concentrated under reduced pressure. Purification by column chromatography in 100% hexanes yielded the product as a bright yellow solid (420 mg, 69% yield): ^{1}H NMR (400 MHz, $CDCl_3$) d 7.01 (m, 4H), d 6.97 (d, J = 3.8 Hz, 2H), d 2.52 (s, 6H); ^{13}C NMR (400 MHz, $CDCl_3$) δ 131.88, 124.44, 123.95, 22.23; LRMS (APCI+) calculated for $C_{14}H_{12}S_5$ 340.57, found 341.25.

*5,5‴Bisthiomethyl 2,2′:5′,2″:5″,2‴-quaterthiophene (**T4**).* The title compound was prepared on a 0.62 mmol scale according to the procedure for compound **T3** with the following modifications: 5,5′-dibromo 2,2′-bithiophene (200 mg, 0.62 mmol, 1 equiv) was used instead of 2,5-dibromothiophene. After heating overnight the product had crashed out of solution. This orange solid was filtered off, washed with methylene chloride, and recrystallized from $CHCl_3$ to yield pure product (158 mg, 60% yield): ^{1}H NMR (400 MHz, $CDCl_3$) d 7.07 (d, J = 3.7 Hz, 2H), d 7.04 (d, J = 3.7 Hz, 2H), d 7.01 (d, J = 3.6 Hz, 2H), d 6.97 (d, J = 3.6 Hz, 2H), d 2.52 (s, 6H); LRMS (EI+) calculated for $C_{18}H_{14}S_6$ 422.69, found 422.2.

5-Thiomethyl-5′-tributylstannyl-2,2′bithiophene. The title compound was prepared according to published procedures,[25] with the following modifications: 5,5′-dibromo 2,2′-bithiophene was used instead of 2,5-dibromothiophene. The product was yielded as a yellow oil (610 mg, 75% yield): ^{1}H NMR (300 MHz, $CDCl_3$) d 7.25 (d, J = 3.4 Hz, 1H), 7.05 (d, J = 3.4 Hz, 1H), 7.01 (d, J = 3.7 Hz, 1H), 6.98 (d, J = 3.7 Hz, 1H), 2.50 (s, 3H), 1.63−1.55 (m, 8H), 1.42−1.34 (m, 8H), 1.17−1.11 (m, 8H), 0.90 (t, J = 7.3 Hz, 12H); ^{13}C NMR (400 MHz, $CDCl_3$) δ 136.23, 132.09, 125.08, 123.61, 29.09, 27.39, 22.38, 13.80, 11.05; HRMS (ESI+) calculated for $C_{21}H_{34}S_3Sn$ 501.40, found 501.97.

*5,5‴″-Dithiomethyl-3″,4″-dihexyl-2,2′,5′,2″,5″,2‴,5‴,2‴″-pentathiophene (**T5**).* The title compound was prepared on a 0.37 mmol scale according to the procedure for compound **T3** with the following modifications: 3,4-dihexyl-2,5-dibromothiophene[26] (150 mg, 0.37 mmol, 1 equiv) was used instead of 2,5-dibromothiophene. 5-Thiomethyl-5′-tributylstannyl-2,2′bithiophene (367 mg, 0.73 mmol, 2 equiv) was used instead of 2-tributylstannyl-5-thiomethyl-thiophene. Purification by column chromatography in 100% hexanes (R_f = 0.19) yielded the product as a bright orangey-red solid (190 mg, 38% yield): ^{1}H NMR (400 MHz, $CDCl_3$) d 7.08 (d, J = 3.8 Hz, 2H), 7.03 (d, J = 2.9 Hz, 2H), 7.02 (d, J = 2.9 Hz, 2H), 6.99 (d, J = 3.7 Hz, 2H), 2.70 (t, 4H), 2.51 (s, 6H), 1.61−1.57 (m, 4H), 1.45−1.40 (m, 4H), 1.34−1.31 (m, 8H), 0.90 (t, 6H); ^{13}C NMR (400 MHz, $CDCl_3$) δ 140.50, 139.32, 136.68, 135.30, 131.90, 129.80, 126.41, 124.05, 123.73, 31.59, 30.72, 29.70, 28.34, 22.76, 22.24, 14.24; LRMS (APCI+) calculated for $C_{34}H_{40}S_7$ 673.14, found 672.3.

*5,5‴″′-Dithiomethyl-3″,4‴-dihexyl-2,2′,5′,2″,5″,2‴,5‴,2‴″,5⁗,2⁗′-sexithiophene (**T6**).* The title compound was prepared on a 0.32 mmol scale according to the procedure for compound **T3** with the following modifications: 5,5′-dibromo-4,4′-dihexyl-2,2′-bithiophene[27] (80 mg, 0.16 mmol, 1 equiv) was used instead of 2,5 dibromothiophene, and 5-thiomethyl-5′-tributylstannyl-2,2′bithiophene (163 mg, 0.32 mmol, 2 equiv) was used instead of 2-tributylstannyl-5-thiomethyl-thiophene. Column chromatography in 10% ethyl acetate in hexanes (R_f = 0.13) yielded the product as a bright red solid (51 mg, 41% yield): ^{1}H NMR (400 MHz, $CDCl_3$) d 7.07 (s, 2H), 7.03 (d, J = 1.0 Hz, 4H), 7.00 (d, J = 1.0 Hz, 4H), 2.70 (t, 4H), 2.52 (s, 6H), 1.73−1.61 (m, 4H), 1.45−1.30 (m, 12H), 0.91 (t, 6H); ^{13}C NMR (500 MHz, $CDCl_3$) d 140.99, 139.53, 137.02, 136.92, 135.44, 135.26, 132.16, 129.76, 126.96, 126.67, 124.37, 124.07, 32.01, 30.78, 29.87, 29.58, 22.96, 22.47, 14.44; LRMS (APCI+) calculated for $C_{38}H_{42}S_8$ 754.11, found 754.5.

*5,5⁗″-Bis(methylthio)-2,2′:5′,2″:5″,2‴:5‴,2⁗″-quinquethiophene (**T5** without hexyl chains).* The title compound was prepared on a 1.62 mmol scale according to the procedure for compound **T3** with the following modifications: 5,5″-dibromo-2,2′:5′,2″-terthiophene (658 mg, 1.62 mmol, 1 equiv) was used instead of 2,5 dibromothiophene. Column chromatography in 10% DCM in hexanes (R_f = 0.21) yielded the product as a dark yellow solid (90 mg, 11% yield): ^{1}H NMR (400 MHz, $CDCl_3$) d 7.23, 7.18, 7.08, 7.04, 7.01, 6.99, 2.52 (s, 6H); LRMS (APCI+) calculated for $C_{22}H_{16}S_7$ 504.82, found 504.7.

Coherent Tunneling Model. The transmission function is calculated using standard Green's function techniques, yielding $T(E) = \Gamma^2|G_{L,R}(E)|^2$, where $G_{L,R}(E) = L|(E - H - \Sigma)^{-1}|R$, and all quantities have been defined previously. The energy-dependent transmission coefficient is evaluated at the Fermi energy, which assumes low bias transport. The specific parameters used in the generation of Figure 4 are (in eV) $\varepsilon_H = -0.9$, $t_H = 0.5$, $\varepsilon_s = E_F = 0$, $t_s = 0.7$, and $\Gamma = 3.0$.

■ ASSOCIATED CONTENT

Ⓢ Supporting Information

Single-molecule histograms and UV−vis spectra. This material is available free of charge via the Internet at http://pubs.acs.org.

■ AUTHOR INFORMATION

Corresponding Authors

lv2117@columbia.edu
lcampos@columbia.edu

Author Contributions

§B. Capozzi and E. J. Dell contributed equally.

Notes

The authors declare no competing financial interest.

■ ACKNOWLEDGMENTS

The authors thank Kateri DuBay for useful discussions. The experimental portion of this work was supported by the NSF (DMR-1206202). The computational work was funded by the Center for Re-Defining Photovoltaic Efficiency through Molecule Scale Control, an EFRC funded by the US Department of Energy, Office of Basic Energy Sciences under Contract No. DE-SC0001085. E.J.D. thanks the HHMI and Dow Chemical Company for International Research Fellowships. T.C.B. was supported by a fellowship from the DOE (SCGF) under Contract No. DE-AC05-06OR23100.

■ REFERENCES

(1) (a) Perepichka, I. F.; Perepichka, D. F. *Handbook of Thiophene-Based Materials: Applications in Organic Electronics and Photonics*; Wiley: Chichester, U.K., 2009. (b) Dennler, G.; Scharber, M. C.; Brabec, C. J. *Adv. Mater.* **2009**, *21*, 1323. (c) Sirringhaus, H.; Tessler, N.; Friend, R. H. *Science* **1998**, *280*, 1741. (d) Sirringhaus, H.; Brown, P. J.; Friend, R. H.; Nielsen, M. M.; Bechgaard, K.; Langeveld-Voss, B. M. W.; Spiering, A. J. H.; Janssen, R. A. J.; Meijer, E. W.; Herwig, P.; de Leeuw, D. M. *Nature* **1999**, *401*, 685. (e) Roncali, J. *Chem. Rev.* **1992**, *92*, 711. (f) Treat, N. D.; Campos, L. M.; Dimitriou, M. D.; Ma, B. W.; Chabinyc, M. L.; Hawker, C. J. *Adv. Mater.* **2010**, *22*, 4982.

(2) Henson, Z. B.; Mullen, K.; Bazan, G. C. *Nat. Chem.* **2012**, *4*, 699.

(3) Zhang, L.; Colella, N. S.; Liu, F.; Trahan, S.; Baral, J. K.; Winter, H. H.; Mannsfeld, S. C. B.; Briseno, A. L. *J. Am. Chem. Soc.* **2012**, *135*, 844.

(4) Koch, F. P. V.; Heeney, M.; Smith, P. *J. Am. Chem. Soc.* **2013**, *135*, 13699.

(5) (a) Xu, B. Q.; Li, X. L.; Xiao, X. Y.; Sakaguchi, H.; Tao, N. J. *Nano Lett.* **2005**, *5*, 1491. (b) Yamada, R.; Kumazawa, H.; Noutoshi, T.; Tanaka, S.; Tada, H. *Nano Lett.* **2008**, *8*, 1237. (c) Leary, E.; Höbenreich, H.; Higgins, S. J.; van Zalinge, H.; Haiss, W.; Nichols, R. J.; Finch, C. M.; Grace, I.; Lambert, C. J.; McGrath, R.; Smerdon, J. *Phys. Rev. Lett.* **2009**, *102*, 086801.

(6) (a) Leary, E.; Hobenreich, H.; Higgins, S. J.; van Zalinge, H.; Haiss, W.; Nichols, R. J.; Finch, C. M.; Grace, I.; Lambert, C. J.; McGrath, R.; Smerdon, J. *Phys. Rev. Lett.* **2009**, *102*, 086801. (b) Xu, B. Q.; Li, X. L.; Xiao, X. Y.; Sakaguchi, H.; Tao, N. J. *Nano Lett.* **2005**, *5*, 1491.

(7) (a) Ie, Y.; Endou, M.; Lee, S. K.; Yamada, R.; Tada, H.; Aso, Y. *Angew. Chem., Int. Ed.* **2011**, *50*, 11980. (b) Lee, S. K.; Yamada, R.; Tanaka, S.; Chang, G. S.; Asai, Y.; Tada, H. *ACS Nano* **2012**, *6*, 5078. (c) Yamada, R.; Kumazawa, H.; Noutoshi, T.; Tanaka, S.; Tada, H. *Nano Lett.* **2008**, *8*, 1237.

(8) Dell, E. J.; Capozzi, B.; DuBay, K. H.; Berkelbach, T. C.; Moreno, J. R.; Reichman, D. R.; Venkataraman, L.; Campos, L. M. *J. Am. Chem. Soc.* **2013**, *135*, 11724.

(9) (a) Gélinas, S.; Rao, A.; Kumar, A.; Smith, S. L.; Chin, A. W.; Clark, J.; van der Poll, T. S.; Bazan, G. C.; Friend, R. H. *Science* **2014**, *343*, 512. (b) Brédas, J.-L.; Norton, J. E.; Cornil, J.; Coropceanu, V. *Acc. Chem. Res.* **2009**, *42*, 1691.

(10) (a) Xu, B. Q.; Tao, N. J. J. *Science* **2003**, *301*, 1221. (b) Venkataraman, L.; Klare, J. E.; Nuckolls, C.; Hybertsen, M. S.; Steigerwald, M. L. *Nature* **2006**, *442*, 904.

(11) Kamenetska, M.; Koentopp, M.; Whalley, A.; Park, Y. S.; Steigerwald, M.; Nuckolls, C.; Hybertsen, M.; Venkataraman, L. *Phys. Rev. Lett.* **2009**, *102*, 126803.

(12) Gonzalez, M. T.; Wu, S. M.; Huber, R.; van der Molen, S. J.; Schonenberger, C.; Calame, M. *Nano Lett.* **2006**, *6*, 2238.

(13) (a) Engelkes, V. B.; Beebe, J. M.; Frisbie, C. D. *J. Am. Chem. Soc.* **2004**, *126*, 14287. (b) Chen, W.; Widawsky, J. R.; Vázquez, H.; Schneebeli, S. T.; Hybertsen, M. S.; Breslow, R.; Venkataraman, L. *J. Am. Chem. Soc.* **2011**, *133*, 17160. (c) Meisner, J. S.; Kamenetska, M.; Krikorian, M.; Steigerwald, M. L.; Venkataraman, L.; Nuckolls, C. *Nano Lett.* **2011**, *11*, 1575.

(14) (a) Park, Y. S.; Whalley, A. C.; Kamenetska, M.; Steigerwald, M. L.; Hybertsen, M. S.; Nuckolls, C.; Venkataraman, L. *J. Am. Chem. Soc.* **2007**, *129*, 15768. (b) Li, C.; Pobelov, I.; Wandlowski, T.; Bagrets, A.; Arnold, A.; Evers, F. *J. Am. Chem. Soc.* **2008**, *130*, 318. (c) Beebe, J. M.; Engelkes, V. B.; Miller, L. L.; Frisbie, C. D. *J. Am. Chem. Soc.* **2002**, *124*, 11268. (d) Hybertsen, M. S.; Venkataraman, L.; Klare, J. E.; Whalley, A. C.; Steigerwald, M. L.; Nuckolls, C. *J. Phys.: Condens. Matter* **2008**, *20*, 374115. (e) Akkerman, H. B.; de Boer, B. *J. Phys.: Condens. Matter* **2008**, *20*, 013001. (f) Salomon, A.; Cahen, D.; Lindsay, S.; Tomfohr, J.; Engelkes, V. B.; Frisbie, C. D. *Adv. Mater.* **2003**, *15*, 1881.

(15) (a) He, J.; Chen, F.; Li, J.; Sankey, O. F.; Terazono, Y.; Herrero, C.; Gust, D.; Moore, T. A.; Moore, A. L.; Lindsay, S. M. *J. Am. Chem. Soc.* **2005**, *127*, 1384. (b) Davis, W. B.; Svec, W. A.; Ratner, M. A.; Wasielewski, M. R. *Nature* **1998**, *396*, 60.

(16) D'Andrade, B. W.; Datta, S.; Forrest, S. R.; Djurovich, P.; Polikarpov, E.; Thompson, M. E. *Org. Electron.* **2005**, *6*, 11.

(17) (a) Meisner, J. S.; Kamenetska, M.; Krikorian, M.; Steigerwald, M. L.; Venkataraman, L.; Nuckolls, C. *Nano Lett.* **2011**, *11*, 1575. (b) Cheng, Z. L.; Skouta, R.; Vazquez, H.; Widawsky, J. R.; Schneebeli, S. T.; Chen, W.; Hybertsen, M. S.; Breslow, R.; Venkataraman, L. *Nat. Nanotechnol.* **2011**, *6*, 353.

(18) Le, Y.; Endou, M.; Lee, S. K.; Yamada, R.; Tada, H.; Aso, Y. *Angew. Chem., Int. Ed.* **2011**, *50*, 11980.

(19) (a) Curtis, M. D.; Cao, J.; Kampf, J. W. *J. Am. Chem. Soc.* **2004**, *126*, 4318. (b) Horowitz, G.; Bachet, B.; Yassar, A.; Lang, P.; Demanze, F.; Fave, J. L.; Garnier, F. *Chem. Mater.* **1995**, *7*, 1337. (c) Siegrist, T.; Fleming, R. M.; Haddon, R. C.; Laudise, R. A.; Lovinger, A. J.; Katz, H. E.; Bridenbaugh, P.; Davis, D. D. *J. Mater. Res.* **1995**, *10*, 2170.

(20) (a) Leclere, P.; Surin, M.; Viville, P.; Lazzaroni, R.; Kilbinger, A. F. M.; Henze, O.; Feast, W. J.; Cavallini, M.; Biscarini, F.; Schenning, A. P. H. J.; Meijer, E. W. *Chem. Mater.* **2004**, *16*, 4452. (b) Ellinger, S.; Ziener, U.; Thewalt, U.; Landfester, K.; M?ller, M. *Chem. Mater.* **2007**, *19*, 1070. (c) Ellinger, S.; Kreyes, A.; Ziener, U.; Hoffmann-Richter, C.; Landfester, K.; M?ller, M. *Eur. J. Org. Chem.* **2007**, 5686. (d) Nepomnyashchii, A. B.; Ono, R. J.; Lyons, D. M.; Sessler, J. L.; Bielawski, C. W.; Bard, A. J. *J. Phys. Chem. Lett.* **2012**, *3*, 2035.

(21) Arroyo, C. R.; Leary, E.; Castellanos-Gómez, A. s.; Rubio-Bollinger, G.; González, M. T.; Agraït, N. s. *J. Am. Chem. Soc.* **2011**, *133*, 14313.

(22) Vazquez, H.; Skouta, R.; Schneebeli, S.; Kamenetska, M.; Breslow, R.; Venkataraman, L.; Hybertsen, M. S. *Nat. Nanotechnol.* **2012**, *7*, 663.

(23) Yoshizawa, K.; Tada, T.; Staykov, A. *J. Am. Chem. Soc.* **2008**, *130*, 9406.

(24) Chi, C. C.; Pai, I. F.; Chung, W. S. *Tetrahedron* **2004**, *60*, 10869.

(25) Barbarella, G.; Zambianchi, M.; Ventola, A.; Fabiano, E.; Della Sala, F.; Gigli, G.; Anni, M.; Bolognesi, A.; Polito, L.; Naldi, M.; Capobianco, M. *Bioconjugate Chem.* **2006**, *17*, 58.

(26) Zhang, W.; Moore, J. S. *Macromolecules* **2004**, *37*, 3973.

(27) Takahashi, M.; Masui, K.; Sekiguchi, H.; Kobayashi, N.; Mori, A.; Funahashi, M.; Tamaoki, N. *J. Am. Chem. Soc.* **2006**, *128*, 10930.